THE MODEL OF LINEAR AGGREGATE OF Ag COLLOIDAL PARTICLES WITH VARIABLE INTER-PARTICLE DISTANCES

Ondrej SESTAK, Pavel MATEJKA* and Blanka VLCKOVA**

Department of Physical and Macromolecular Chemistry,
Charles University, 128 40 Prague 2, Czech Republic

A simplified method of calculation of the surface plasmon energy states of the Ag colloidal aggregates characterized by varying inter-particle (inter-sphere) distance has been developed. Ag colloidal aggregate is approximated by a linear (one-dimensional) assembly of N silver spheres (of identical radii r and identical inter-sphere distances D) mutually interacting by a dipole–dipole interaction. The calculations use the following parameters: N from 1 to 25, $r = 2, 5$ and 10 nm, $D = 0$, 0.5, 1 and 2 nm, water and/or vacuum embedding media. The perturbation energies V_{min} (stabilization energy) and V_{max} (destabilization energy) of the excited plasmon state of a linear aggregate of N spheres interacting by the dipole–dipole interaction were calculated as the eigenvalues of perturbation matrix using the above-mentioned parameters. The stabilization energy V_{min} increases with increasing number of spheres in the aggregate and with increasing sphere radius, while it decreases with increasing inter-particle (inter-sphere) distance. Calculations of the square values of the eigenvector coefficients show that the contribution of a particular single sphere to the total energy of the aggregate is the highest for the central sphere in the odd-N aggregates and for the two central spheres in the even-N aggregates. The results of the model calculations support the hypothesis that the differences between the surface plasmon absorption curves of the Ag colloid/monomeric adsorbate and of the Ag colloid/polymeric (oligomeric) adsorbate systems have their origin in the difference in the inter-particle distance distributions.

Key words: Ag-colloid; Linear aggregates; Aggregation theory, SERS; Surface plasmon states.

Ag colloids are suitable model systems for investigation of the electromagnetic mechanism of SERS (Surface Enhanced Raman Scattering) chiefly because of the possibility to follow the surface plasmon absorption (SPA) of the Ag colloid/adsorbate system by UV/VIS absorption spectroscopy. The changes in the SPA of Ag colloid upon aggregation were explained theoretically by the Fornasiero–Grieser's model of linear aggregate of Ag colloidal particles[1]. For a linear aggregate of Ag particles interacting by a di-

---

pole–dipole interaction, two excited surface plasmon states originate and two absorption bands, one at lower energy than the monomer (single particle) absorption band, the other at a higher energy, are observed. Differences in the SPA spectra of SERS active systems with different adsorbates are ascribed to a varying degree of the Ag colloid aggregation[2]. In our previous studies[3–6], we found systematical differences in the SPA spectra of SERS-active systems containing polymeric (i.e. proteins[4]) and/or oligomeric (i.e. polypeptide[3], Triton X-100 (refs[5,6])) species in comparison to the spectra of systems formed by monomeric species. In this paper, we first introduce the hypothesis which provides a possible explanation of the differences between the SPA curves of the Ag colloid/monomeric adsorbate systems and those of Ag colloid/polymeric (oligomeric) systems. Furthermore, in order to verify our hypothesis, we present here the results of the calculations of the energy states of a linear colloidal aggregate.

HYPOTHESIS

The second maximum of plasmon absorption, which is observed in systems containing species of monomeric nature in the 540–620 nm range, is ascribed to SPA of the aggregates of spherical colloidal particles. In contrast to that, for SERS-active systems containing species of polymeric character, only an asymmetric broadening of the original monomer (single particle) peak towards higher wavelengths is typical (without appearance of a pronounced second maximum). Up to now, no explanation concerning the origin of a different character of the plasmon absorption curves for systems formed by polymeric (oligomeric) and monomeric species has been published. On the basis of our previous results[3–6], we introduce here a hypothesis, that differences between plasmon absorption curves are given by different distances of Ag colloidal particles in the aggregates. We assume that for the monomeric adsorbates, the colloidal particles in aggregates are almost in touch with each other ($D = 0$ nm), while for aggregates formed by polymeric or oligomeric species, non-zero distances between individual spheres (Ag colloidal particles) have to be considered. To verify this hypothesis, we have developed a new model of colloidal aggregate which combines Aravind's and Fornasiero's theoretical approaches[1,7]. The model describes a linear aggregate of spheres (Ag colloidal particles) mutually interacting by a dipole–dipole interaction in which the inter-sphere distances are generally non-zero and are involved as an adjustable parameter in the calculations of the energy states of the aggregate. In our calculation, the dipole–dipole interactions of the spheres in the linear aggregate are considered as a perturbation affecting the energy of the excited plasmon state of an assembly of N non-interacting spheres and is expressed in terms of the perturbation operator $\hat{V}$. The perturbation energies V_{min} (stabilization energy) and V_{max} (destabilization energy) of the excited plasmon state of a linear aggregate of N spheres interacting by the dipole–dipole interactions will be calculated as eigenvalues of the perturbation matrix (the matrix representation of the perturbation operator $\hat{V}$). The V_{min} values will thus represent the stabilization

energy of the excited plasmon state of the longitudinal plasmon mode of the linear aggregate of N interacting spheres with respect to the degenerate excited plasmon state of an assembly of N non-interacting spheres.

THEORETICAL

The model of linear colloidal aggregate is based on the following assumptions:

1. only dipolar interactions between colloidal particles in the aggregate are considered;

2. the radii of all colloidal particles are identical;

3. the distances between adjacent spheres (colloidal particles) are identical;

4. the aggregate axis is oriented along the *x*-axis.

The vector of distances $\overrightarrow{R_{ij}}$ between the centers of individual spheres (*i* and *j*) can thus be described by Eq. (*1*):

$$\overrightarrow{R_{ij}} = (2r + D)\,(j - i)\,\overrightarrow{k}, \tag{1}$$

where r is the sphere radius, D is the distance between adjacent spheres and $\overrightarrow{k}$ is the unitary vector ($|\overrightarrow{k}| = 1$) oriented in direction of the aggregate axis.

5. The longitudinal plasmon mode[1] is oriented along x axis and the transversal modes are oriented along the y and z axis, respectively.

The individual dipolar interaction energies V_{ij} (between each two individual spheres i and j, $i \neq j$) are described by Eq. (*2*):

$$V_{i,j} = \frac{1}{4\pi\varepsilon_{e}}\,\frac{1}{(|\overrightarrow{R_{ij}}|)^3}\left[\overrightarrow{\mu_i}\,\overrightarrow{\mu_j} - \frac{3(\overrightarrow{R_{ij}}\,\overrightarrow{\mu_i})\,(\overrightarrow{R_{ij}}\,\overrightarrow{\mu_j})}{|\overrightarrow{R_{ij}}|^2}\right], \tag{2}$$

where $\overrightarrow{R_{ij}}$ is defined as above and $\overrightarrow{\mu}$ is the induced dipole moment for a single sphere[1,8,14], where ε_{e}, the dielectric function of environment, is the product of the permittivity of vacuum ε_0 and relative permittivity of environment ε_{r}. The induced dipole moment for a single sphere $\overrightarrow{\mu}$ can be described by Eq. (*3*):

$$\overrightarrow{\mu} = 4\pi\varepsilon_{e}\left(\frac{\varepsilon(\omega) - 1}{\varepsilon(\omega) + 2}\right)r^3\,\overrightarrow{E}(\omega), \tag{3}$$

where $\overrightarrow{E}$ is a vector of the intensity of the incident electric field and $\varepsilon(\omega)$ is the dielectric function of silver[8].

With these equations we have developed a new formula for dipolar interaction energy of a single sphere (Eq. (*4*)): (The details of formulation of Eq. (*4*) are given in Appendix).

$$V_{i,j} = \frac{8\pi}{c} \, \varepsilon_{\mathrm{r}} \left(\frac{(n^2 - k^2)\,(n^2 - k^2 - 2) + 1}{(n^2 - k^2)\,(n^2 - k^2 + 4) + 4} \right) \frac{r^6}{|(2r + D)\,(j - i)|^3} \cdot$$

$$\cdot \cos\left[\frac{2\pi}{\lambda}\,(2r + D)\,(i + j - 2)\,(\sin(\theta)\cos(\varphi) - 1) \right] [1 - 3\sin^2(\theta)\cos^2(\varphi)]\,I \ , \quad (4)$$

where c is the velocity of light in vacuum, n is the refractive index, k is the absorption coefficient (n and k are referred to as "bulk constants" (ref.[8])) for Ag and depend on the wavelength of incident radiation), λ is the wavelength of incident radiation, θ, φ are the angles of incidence (in spherical coordinates), I is the intensity of the incident radiation.

The individual values $V_{i,j}$ form a perturbation matrix V of the N-th order for the particular N-membered colloidal aggregate. This perturbation matrix is the matrix-representation of perturbation operator $\hat{V}$ of the overall energy of aggregate. The eigenvalues of this perturbation matrix have to be calculated[9] to determine the energy states of aggregate. The least square method[10] was used for the calculation of the largest eigenvalue of the perturbation matrix. Furthermore, to obtain the contributions of the individual spheres in the aggregate to its total energy, we calculate the normalized eigenvectors of the perturbation operator belonging to the particular eigenvalues of energy. Squares of eigenvector coefficients determine the contribution of each individual sphere to the total energy of aggregate[9]. For angles of incidence θ, $\varphi = 90°$, $0°$ the solution describes the energy level of the longitudinal plasmon mode ($V_{\min}$), while for angles of incidence θ, $\varphi = 0°$, $90°$ and $0°$, $0°$ the solution gives the energy levels of the transversal plasmon modes $V_{\max}$ (the linear colloidal aggregate is oriented along x axis). A necessary step in our calculation was evaluation of the square values of induced dipole moment $|\vec{\mu}|^2$ in dependence on the wavelength of incident radiation Eq. (*5*):

$$|\vec{\mu}|^2 = \frac{32\pi^2}{c} \, \varepsilon_{\mathrm{e}}\varepsilon_{\mathrm{r}} \left(\frac{(n^2 - k^2)\,(n^2 - k^2 - 2) + 1}{(n^2 - k^2)\,(n^2 - k^2 + 4) + 4} \right) r^6 I \ . \tag{5}$$

RESULTS OF CALCULATIONS

The square values of the induced dipole moment of a silver sphere as a function of the wavelengths of the incident radiation are shown in Figs 1 and 2. The maximum of the square values of the induced dipole moment for a 5 nm sphere embedded in water is located at 375 nm (Fig. 1), while for the sphere of the same radius embedded in vacuum, the corresponding maximum is at 355 nm (Fig. 2). The shift of the maximum of the square values of the induced dipole moment for a sphere embedded in water in

comparison to that embedded in vacuum has its origin in the different values of permittivity ε_0 and permeability μ_0 for water and vacuum, and is in a good agreement with the results published[11]. The same maxima of the square values of the induced dipole moments were obtained also for the 2 nm and 10 nm spheres. The deviation of the calculated value (375 nm) from the real value[11] (390 nm) is most probably caused by the fact, that particles of the real Ag colloid are embedded in an "electrolyte" with a higher ionic strength than that of pure water. The presence of BH_4^- and BO_3^- ions in SERS-active system results from the procedure of preparation of Ag colloid[12]. The existence and stability of isolated Ag particles is conditioned by the existence of an electric bilayer on the surface of each colloidal particle[13]. The calculated values of wavelengths (375 nm for water, 355 nm for vacuum) at which the squares of induced dipole moment reach their maxima were used for selection of input parameters ("bulk constants" for Ag (ref.[8])) to the following model calculations.
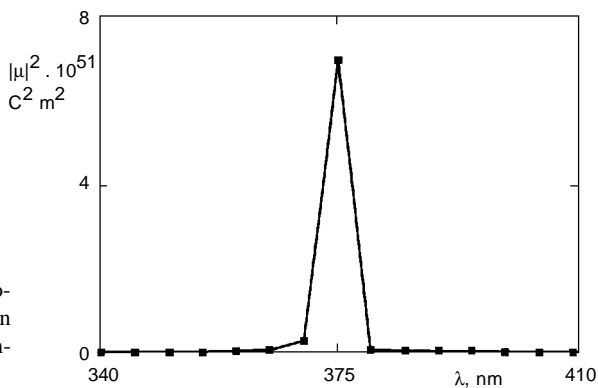

FIG. 1

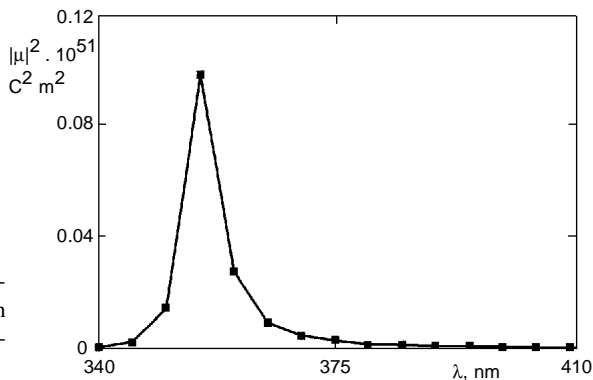Square values of the induced dipole moment μ as a function of the excitation wavelength λ for 5 nm sphere embedded in water

FIG. 2

Square values of the induced dipole moment μ as a function of the excitation wavelength λ for 5 nm sphere embedded in vacuum

The square values of eigenvector coefficients were calculated to determine the contribution of the particular single sphere to the energy states of the colloidal aggregate[9]. The dependence of the squares of eigenvector coefficients on the position number of the sphere in the aggregate (N) is shown in Figs 3 and 4. The Figs 3 and 4 show the
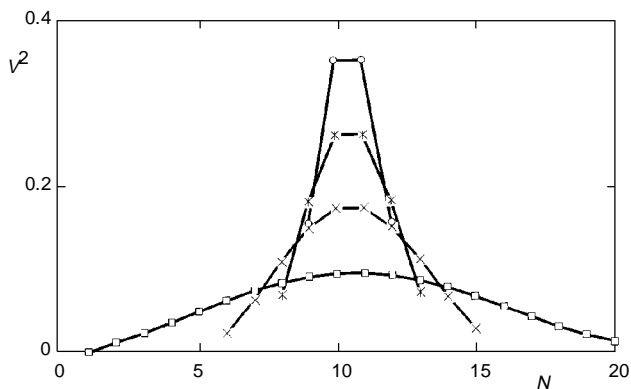

F<small>IG</small>. 3

The dependence of the square values of the eigenvector coefficients (V^2) on the position numbers of the spheres (N) in the even membered aggregate of twenty spheres (5 nm sphere radius, 2 nm inter-sphere distance, aggregates embedded in water and excited by 375 nm radiation). The same dependence is depicted also for other even membered aggregates: ❏ $N = 20$, × $N = 10$, ✱ $N = 6$, ◯ $N = 4$. For the sake of comparison, the centres of 4, 6, 10 membered aggregates are located into the central positions of the spheres of the 20 membered aggregate (position numbers $N = 10, 11$)
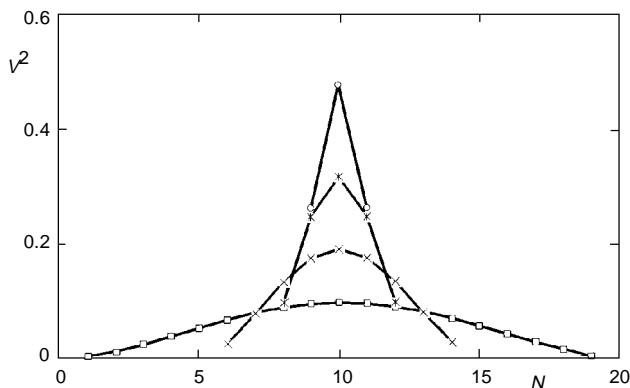

F<small>IG</small>. 4

The dependence of the square values of the eigenvector coefficients (V^2) on the position numbers of the spheres (N) in the odd membered aggregate of nineteen spheres (5 nm sphere radius, 2 nm inter-sphere distance, aggregates embedded in water and excited by 375 nm radiation). The same dependence is depicted also for other even membered aggregates: ❏ $N = 19$, × $N = 9$, ✱ $N = 5$, ◯ $N = 3$. For the sake of comparison, the centres of 3, 5, 9 membered aggregates are located into the central positions of the spheres of the 19 membered aggregate (position numbers $N = 10$)

dependences for the even/odd membered aggregates. Our calculations show that the highest contribution from a single sphere to the total energy states of the aggregate arises: (i) in the case of even sphere-numbers from the two spheres which are located in the centre of the aggregate, and (ii) in the case of odd sphere-numbers from the sphere located in the center of the aggregate. The values of squares of the eigenvector coefficients are independent of the wavelength of incident radiation, the radii of
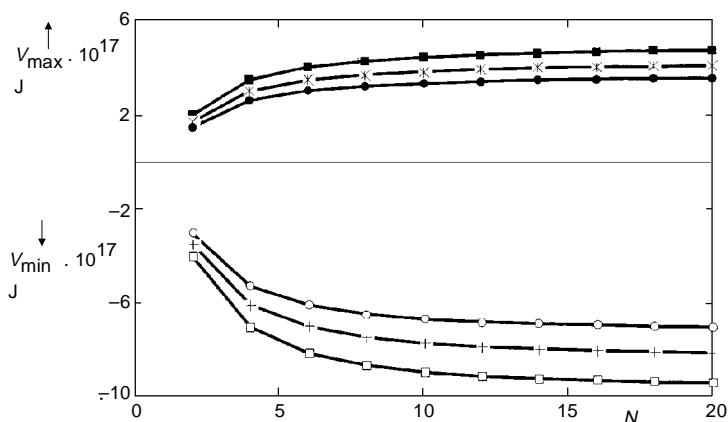

Fig. 5

Dependence of the energies V_{min} and V_{max} on the position number of the spheres (N) in aggregate at varying inter-sphere distances D (in nm) of the 5 nm spheres embedded in water and excited by 375 nm radiation. $\square$ $D = 0$, V_{min}; $+$ $D = 0.5$, V_{min}; $\bigcirc$ $D = 1$, V_{min}; $\blacksquare$ $D = 0$, V_{max}; $\ast$ $D = 0.5$, V_{max}; $\bullet$ $D = 1$, V_{max}
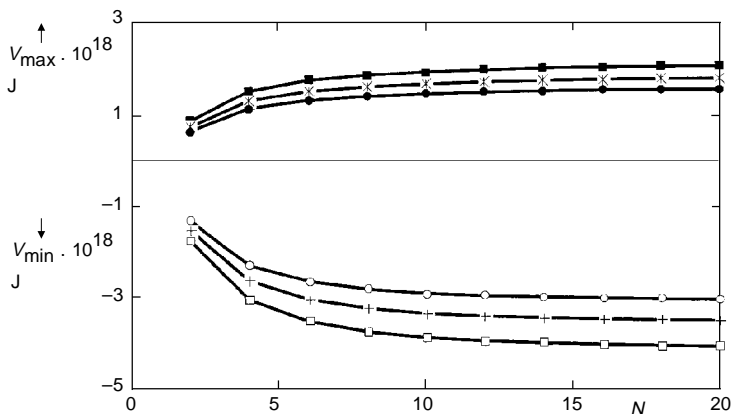

Fig. 6

Dependence of the energies V_{min} and V_{max} on the position number of the spheres (N) in aggregate at varying inter-sphere distances D (in nm) of the 5 nm spheres embedded in vacuum and excited by 355 nm radiation. $\square$ $D = 0$, V_{min}; $+$ $D = 0.5$, V_{min}; $\bigcirc$ $D = 1$, V_{min}; $\blacksquare$ $D = 0$, V_{max}; $\ast$ $D = 0.5$, V_{max}; $\bullet$ $D = 1$, V_{max}

spheres, and the distances between adjacent spheres. Their values depend only on either the odd or the even numbers of spheres in the aggregate. The nondependence of squares of eigenvector coefficients on the varying distances between adjacent spheres is an important result which indicates formal correctness of the approach adopted in our model of colloidal aggregate.

Finally, we have calculated the eigenvalues of energy for the longitudinal plasmon mode (V_{min}) and for the transversal plasmon modes (V_{max}). The values V_{min} represent the stabilization energies of the aggregate. The dependence of the energies (V_{min}, V_{max}) on the following factors has been calculated:

1. the number of spheres in the aggregate (N)

2. the radius of a single sphere (r)

3. the distance between adjacent spheres in the aggregate (D).

Figures 5 and 6 show the dependences of V_{min}, V_{max} on the number of spheres in the aggregate for varying inter-sphere distances D at constant sphere radii r (r = 5 nm) using n, k values of Ag (ref.[8]) (at 375 nm wavelength of incident radiation for the aggregates embedded in water, and at 355 nm for those embedded in vacuum). Further-more, Figs 5 and 6 show that an increase in the distance between the adjacent spheres in the aggregate leads to a decrease in the absolute values of energies V_{min}, V_{max}. This result can readily be explained by the decrease in the dipole–dipole interaction between the spheres in the aggregate with the increasing inter-sphere distance. Analogous calcu-lations were made for spheres of 2 and 10 nm radii.

CONCLUSIONS

For a linear aggregate consisting of N identical Ag colloidal particles (spheres) mu-tually interacting by a dipole–dipole interaction, the stabilization energy V_{min} of the longitudinal plasmon mode and the "destabilization" energy of the two degenerate transversal plasmon modes V_{max} were calculated as functions of (i) number of spheres in the aggregate; (ii) radius of the spheres; (iii) inter-sphere distance.

The absolute values of V_{min} and V_{max} (i) increase with increasing number of spheres in the aggregate N for $N \leq 15$, but become virtually independent of N for $N \geq 15$; (ii) increase with increasing radius of the spheres; (iii) decrease with increasing inter-sphere distance.

From the results of this model calculation, important conclusions concerning the real Ag colloid/adsorbate systems can be drawn:

1. As Ag colloidal aggregates in real systems consist of more than a hundred Ag particles[15], the number of the spheres in the aggregate cannot significantly influence the shapes of SPA curves of real Ag colloid/adsorbate systems.

2. The size of the Ag colloidal particles significantly influences the energies of the surface plasmon states of the aggregate. The shapes of the SPA curves of real Ag colloid/adsorbate systems thus reflect particle size distributions in these systems.

3. The inter-particle distances significantly influence the energies of the surface plasmon state of the aggregate. For systems with non-zero inter-particle distances, the distribution of the inter-particle distances can substantially influence the shape of the SPA curve of the SERS-active system.

The above conclusions provide a key to explanation of the systematic differences between SPA curves of the SERS-active systems formed by the polymeric (oligomeric) and/or the monomeric adsorbates. For Ag colloidal aggregates formed by monomeric species, the individual spheres are nearly in touch and the inter-sphere distances can be considered to be close to $D = 0$ nm. On the other hand, in the case of polymeric (oligomeric) species, one polymer chain can be adsorbed simultaneously on two or more Ag particles thus preventing them from touching. Therefore, in the Ag colloidal aggregates formed by polymeric species, the distances between the adjacent spheres are non-zero ($D > 0$ nm). Their distribution can be described by a distribution function. Consequently, the shapes of SPA curves of the Ag colloid/monomer systems are governed by only one distribution function describing the distribution of particle sizes, and a well defined maximum in the red spectral region is usually observed. By contrast, the shapes of the SPA curves of Ag colloid/polymer (oligomer) systems are governed by two distribution functions (i) distribution of particle sizes and (ii) distribution of inter-particle distances. This is the reason why the SPA curves of these systems do not show a single, well pronounced maximum, but a broad absorption feature extending from the absorption band of the residual isolated particles towards the red spectral region.

APPENDIX

The dielectric function of the metal $\varepsilon(\omega)$ consists of a real ε_1 and imaginary $i\varepsilon_2$ part which are related to the refractive index n and absorption coefficient k of the metal by the following equations[8]:

$$\varepsilon(\omega) = \varepsilon_1 + i\varepsilon_2$$

$$\varepsilon_1 = n^2 - k^2$$

$$\varepsilon_2 = 2nk \ .$$

By inserting ε_1, the real part of $\varepsilon(\omega)$ into Eq. (*3*) (ref.[11]), we obtain Eq. (*A-1*):

$$\vec{\mu}_{i,j} = 4\pi\varepsilon_e \frac{(n^2 - k^2) - 1}{(n^2 - k^2 + 2)} r^3 \vec{E}_{i,j}(\omega) \ , \tag{A-1}$$

where ε_e is the dielectric function of environment. In our calculation, the aggregate is fixed along the x axis. This assumption means, that the components R_{ij}^y and R_{ij}^z of the vector $\overrightarrow{R}_{ij}$ vanish. Therefore a simplification of Eq. (2) gives Eq. (A-2):

$$V_{i,j} = \frac{1}{4\pi\varepsilon_e} \frac{1}{|(2r+d)\,(j-i)|^3}\,(\mu_i^y\,\mu_j^y + \mu_i^z\,\mu_j^z - 2\mu_i^x\,\mu_j^x)\ . \tag{A-2}$$

Subsequent expansion of this equation with the use of Eq. (A-1) results in Eq. (A-3):

$$V_{i,j} = 4\pi\varepsilon_e\,\frac{r^6}{|(2r+d)\,(j-i)|^3}\left(\frac{(n^2-k^2)\,(n^2-k^2-2)+1}{(n^2-k^2)\,(n^2-k^2+4)+4}\right)\cdot$$
$$\cdot\,(E_i^y E_j^y + E_i^z E_j^z - 2E_i^x E_j^x)\ . \tag{A-3}$$

Furthermore we assume that incident plane electromagnetic wave creates the incident electric field intensity $\overrightarrow{E}(\omega)$:

$$\overrightarrow{E}_{i,j}(\omega) = \overrightarrow{E}_{0_{i,j}} \exp\,[i\overrightarrow{k}\overrightarrow{r} - i\omega t]\ .$$

We take only the real part of this expansion[16], Eq. (A-4):

$$\overrightarrow{E}_{i,j} = \overrightarrow{E}_{0_{i,j}} \cos\,[(\overrightarrow{k}\overrightarrow{r} - \omega t]\ . \tag{A-4}$$

Using spherical coordinates for description of the aggregate position, we obtain Eq. (A-5):

$$\overrightarrow{E}_{i,j}(\omega) \equiv \left\{E_{i,j}^x, E_{i,j}^y, E_{i,j}^z\right\}\,;\quad \overrightarrow{E}_{0_{i,j}} \equiv \left\{E_{0_{i,j}}^x, E_{0_{i,j}}^y, E_{0_{i,j}}^z\right\}$$
$$\overrightarrow{k} \equiv \left\{k_x, k_y, k_z\right\}$$
$$E_{0_{i,j}}^x = |E_0|\,\sin\,(\theta)\,\cos\,(\varphi)$$
$$E_{0_{i,j}}^y = |E_0|\,\sin\,(\theta)\,\sin\,(\varphi)$$
$$E_{0_{i,j}}^z = |E_0|\,\cos\,(\theta)\ . \tag{A-5}$$

The aggregate is fixed along the x axis, the vector $\overrightarrow{k}$ has the form: $\overrightarrow{k} \equiv \{k_x, 0, 0\}$, where $k_x = |k|\,\cos\,(\theta)\,\sin\,(\varphi)$; $|k| = 2\pi/\lambda$. The vector $\overrightarrow{r} = \{r_x, 0, 0\}$; $r_x = (2r+D)\,(i+j-2)$. Thus the first term in Eq. (A-4) reads as follows:

$$\cos (\overrightarrow{k} \cdot \overrightarrow{r}) = \frac{2\pi}{\lambda} (2r + D) (i + j - 2) \sin \theta \cos \varphi \ .$$

For description of the term ωt, we assume that $\omega t = \omega(t_i + t_j)$ where t_i and t_j are times when the incident wave is in contact with sphere i or j, respectively. The circular frequency is $\omega = 2\pi c/\lambda$, the time $t_j = t_i + [(2r + D) (j - i)]/c$. We assume the initial time $t_1 = 0$. Thus we obtain $t_i = t_1 + [(2r + D) (i - 1)]/c$. We use these expressions in the term $\omega(t_i + t_j)$ and, consequently, in the equation for the product of plane electromagnetic waves. Thus we obtain Eq. (*A-6*):

$$\overrightarrow{E_i}(\omega) \cdot \overrightarrow{E_j}(\omega) = \cos \left(\frac{2\pi}{\lambda} (2r + D) (i + j - 2) (\sin (\theta) \cos (\varphi) - 1) \right) \cdot$$
$$\cdot ((E_0^y)^2 + (E_0^z)^2 - 2(E_0^x)^2) \ . \tag{A-6}$$

We use equations Eq. (*A-5*) for further expansion of Eq. (*A-6*) and introduce the result into Eq. (*A-3*). By expressing $|E_0^2|$ as $|E_0^2| = 2c\mu_0 I$, where I is the intensity of the incident radiation, we directly obtain the Eq. (*4*).

REFERENCES

 1. Fornasiero D., Grieser F. J.: Chem. Phys. *5*, 3213 (1987).
 2. Creighton J. A.: *Metal Colloids in Surface Enhanced Raman Scattering* (R. K. Chang and T. E. Furtak, Eds), p. 315. Plenum Press, New York 1982.
 3. Cermakova K.: *M.S. Thesis*. Charles University, Prague 1992.
 4. Sestak O.: *M.S. Thesis*. Charles University, Prague 1993.
 5. Matejka P., Vlckova B., Vohlidal J., Pancoska P., Baumruk V.: J. Phys. Chem. *96*, 1361 (1992).
 6. Matejka P.: *Ph.D. Thesis*. Charles University, Prague 1993.
 7. Aravind P. K., Nitzan A., Metiu H.: Surf. Sci. *110*, 189 (1981).
 8. Kreibig U., von Fragstein C.: Z. Phys. *224*, 307 (1969).
 9. Tinoco I.: Radiation Res. *20*, 133 (1963).
10. Ralston A.: *Introduction to the Numerical Mathematics*, p. 514. Academia, Prague 1973.
11. Creighton J. A., Eadon D. G.: J. Chem. Soc., Faraday Trans. *87*, 3881 (1991).
12. Ahern A. M., Garrel R. L.: Anal. Chem. *59*, 2813 (1987).
13. Stockman M. I., Shalaev M., Moskovits M., Botet R., George T. F.: Phys. Rev., B *46*, 2821 (1992).
14. Clippe P., Evrard R., Lucas A. A.: Phys. Rev., B *14*, 1715 (1976).
15. Weitz D. A., Oliveira M.: Phys. Rev. Let. *52*, 1433 (1984).
16. Jackson J. D.: *Classical Electrodynamics*. Wiley & Sons, New York 1975.